Proceedings of OMAE04
23rd International Conference on Offshore Mechanics and Arctic Engineering
June 20-25, 2004, Vancouver, British Columbia, Canada

OMAE2004-51575

AN APPROACH TO CALCULATE THE PROBABILITY OF WAVE IMPACT ON AN FPSO BOW

C. Guedes Soares, R. Pascoal and E.M. Antão

Unit of Marine Technology and Engineering, Technical University of Lisbon
Instituto Superior Técnico, Av. Rovisco Pais, 1049-001 Lisbon, Portugal

A.J. Voogt and B. Buchner

MARIN, Haagsteeg 2, NL-6708 PM Wageningen P.O. Box 28
NL-6700 AA Wageningen, The Netherlands

ABSTRACT

This work aims at characterizing the probability of wave impact and expected impact load on the bow geometry of an FPSO.

In order to determine the instants when impact occurs, an experimental program was performed on a specific bow shape. The bow was instrumented with pressure transducers and the test program, also making use of video recordings, was designed such that it was possible to determine the correlation between undisturbed wave shape and the impact pressure time traces. It has been found that wave impact at the bow is highly correlated with the local wave steepness, which for very high waves has at least second order effects.

A comparison between the probability distributions of local wave steepness of the experimental undisturbed wave time trace and numerical simulations of second order wave theory is provided and it confirmed that the latter is very adequate for calculations.

The experimental results were further used to determine how the probability of impact varies with free surface vertical velocity.

It was found that the significant wave height of the sea state itself does not have significant influence on the result and a regression model is derived for that type of bow.

The proposed model for determining the probability of impact load is based on combining both models. The analytical nature makes it fast and easy to expand to other cases of interest and some example calculations are shown to demonstrate the relative ease of the procedure proposed.

The position of the impact is determined by the non-linear wave crests and the ship motions. The ship motions can be determined based on a linear response to the non-linear waves considered.

INTRODUCTION

The occurrence of wave impact at the bow of FPSOs has been a topic of more advanced dedicated research especially since an impact from a steep fronted wave damaged the bow of the new build Schiehallion FPSO, well above the waterline, on November 1998.

There has been research for design of FPSO bows based on a prescribed probability of greenwater events that should not be exceeded. It has been based on non-linear corrections to results of linear radiation-diffraction codes (Buchner 1998, 2002) or by including some second order corrections (Hellan 2001), because the numerical simulations of these phenomena are still not mature enough to be applied during design.

Guedes Soares et al (2001) conducted a series of experiments on motions of an FPSO model and compared the predictions both with a linear radiation-diffraction code and with a strip theory code showing that in both cases an excellent agreement was obtained. Guedes Soares and Pascoal (2002) have studied the probability distributions of green water on deck and showed that based on a relative motion formulation the predictions of the theory agreed well with the measurements. However their results were obtained with a model with basically vertical sided bow, while the ones of (Buchner 1998, 2002) account for different flare and introduce the corrections for that effect.

The present paper was developed within the SAFE-FLOW project (SAFE-FLOating offshore structures under impact loading of shipped green water and waves), which is funded by the European Community and by a large group of 26 industrial participants (oil companies, shipyards, engineering companies, regulating bodies). Its objective is to develop guidance, calculation methods and risk assessment procedures for green water and wave impact loading appropriate to each stage of a floater project,

namely: concept development, detailed design and operation.

The greenwater and wave impact events are basically of the same type in the sense that they are related to the relative motion between the platform and the waves. However while green water occurs when the waves are high enough to reach the deck or side of the platform, the impact of a bow can occur with waves that are not is high but on the other hand they need to be steep enough for an impact to occur. Therefore while for green water it is the distribution of the relative motion or the distribution of wave crests that are on interest, for the bow impact problem it is the distribution of wave steepness that is governing.

The research reported herein shows how it was concluded that the determining factor for wave slam was the local wave steepness and considers the adequacy of second order wave models to be used for design purposes, to determine the probability of local wave steepness and consequently the probability of wave impact given a sea state and on the position of the impact on the bow.

NOMENCLATURE

a_n - Wave amplitude of the nth Fourier component.
k - Wave number.
w - Free surface vertical velocity.
t - Time.
x - Horizontal coordinate, function variable.
z - Free surface elevation.
γ - JONSWAP peak intensification factor
ω - Wave angular frequency
$\langle x-a \rangle^1 = \begin{cases} 0 & , x \le a \\ x-a & , x > a \end{cases}$ - Ramp Function
PexcBasin - Exceedance probability estimate calculated from the basin simulation.
PexcNum - Exceedance probability estimate calculated from the numerical simulation.

EXPERIMENTAL PROGRAM

In the model test research conducted within the SAFE-FLOW project (Voogt, 2001), it was identified that the wave impact loading on the free floating model of the Schiehallion FPSO was not dominated by relative wave motions effects, but by the local characteristics of the waves themselves. Based on this observation, a second series of model tests was carried out with a simplified fixed bow structure with detailed pressure instrumentation, so that the relation between the waves and the wave impacts could be studied in more detail. Figure 1 shows the details of the schematic bow set-up and its instrumentation. The scale was 1:60.

The tests were carried out in the MARIN Seakeeping and Manoeuvring Basin, which has a depth of 5.0m (model scale). The experimental setup was mounted in a way that made it possible to run physical tests, consisting of generating waves in a basin, such that the wave sequence was very close to being exactly repeatable.

First the waves were generated and measured by several probes mounted at the location where a fixed bow model was to stand, as schematically presented in Figure 2. The probes are mounted in such a way that it is possible to get a good estimate of local free surface steepness and velocity.

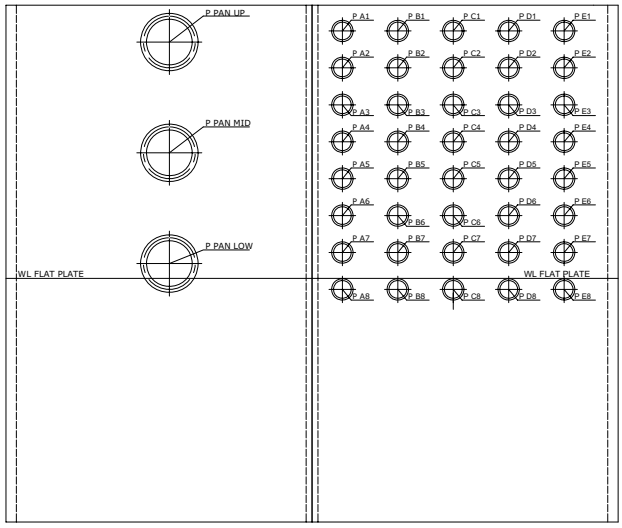

Figure 1.- Front view of schematic bow set-up and its instrumentation.

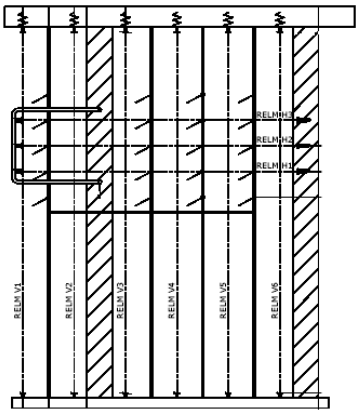

Figure 2.- Schematic of the probe frame.

The wave elevation probes were mounted vertically, parallel to the incoming wave ray, in the case a straight line. There were also probes mounted horizontally in such a manner that the incoming velocity may be more easily calculated.

In the final stage of testing, the sequences were repeated but with the bow model already in position. The bow is instrumented with pressure transducers, as shown in Figure 3, and videotaped so that wave impacts are more easily identified and characterized. Because the wave train is exactly repeatable, it is possible to correlate the events that are to be analysed with the undisturbed wave properties at the time it happens.

Using the undisturbed wave properties, instead of the disturbed, makes it possible to verify if there are some facts closely correlated with the properties of the wave itself and not specific to the bow shape.

The experimental program matrix of tests for wave calibration is presented in Table 1 and each test was repeated 5 times, total of 15hour full scale, with different seeds for the random number generator in order to get better confidence on the values of statistics. The sampling frequency was 25Hz.

JONSWAP				
Hs [m]	Tp [s]	γ	Duration [hrs]	Number of tests
8.0	8.0	3.3	3	5
12.0	12.0	3.3	3	5
14.0	14.0	3.3	3	5

Table 1.- Simulated sea states.

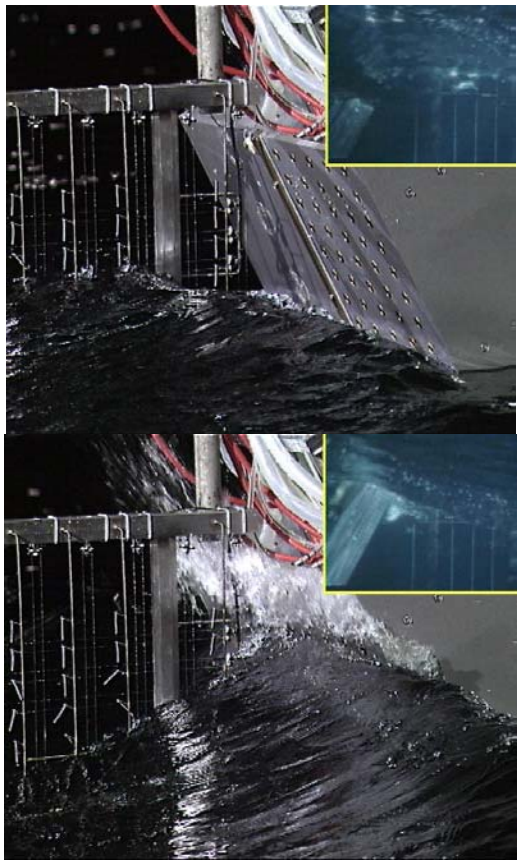

Figure 3.- Wave impact on the instrumented fixed bow (top right corner shows mirrored underwater view).

The impact tests were performed on a flat plate, i.e. 180 degree internal angle, with 15 and 30 degrees tilt and on triangular plates with 30 degree tilt but with internal angles of 150 and 120 degrees, the loads are sampled at a rate of 2000Hz. The test matrices, for irregular waves, are given in Table 2 to Table 4. For the flat plate with 30º tilt, 5 times 3h tests were run using the previously calibrated waves, the different simulations of the same seastate will henceforth be referred to as groups 1, 2 and 3. For the other plates, only the signal around the strongest impact was used and repeated 10 times.

Flat Plate (180º internal angle)					
Hs [m]	Tp [s]	γ	Duration [hrs]	Number of tests	Group of tests
8.0	8.0	3.3	3	5	1
12.0	12.0	2.5	3	5	2
14.0	14.0	2.0	3	5	3

Table 2.- Impact on flat plate with 30º tilt.

Flat Plate (180º internal angle)				
Hs [m]	Tp [s]	γ	Duration [hrs]	Number of tests
14.0	14.0	2.0	0.25	10

Table 3.- Impact on flat plate with 15º tilt.

Triangular Plates (150º & 120º internal angles)				
Hs [m]	Tp [s]	γ	Duration [hrs]	Number of tests
14.0	14.0	2.0	3	1
14.0	14.0	2.0	0.25	1

Table 4.- Impact on triangular plate with 30º tilt.

ANALYSIS OF EXPERIMENTAL RESULTS

The test data that is analysed herein is only relative to the flat plate with 30º tilt. The wave, pressure and video time traces are analysed on a wave by wave basis. The impact events are identified and it is studied how the impact pressures propagate and how the impulse changes. The height at which the impact occurs was registered and the impact conditions were determined. By detailed analysis of the tests, it was found that the impulse of the wave impact was governed by the maximum local free surface steepness (Voogt, 2004).

The local free surface steepness is linearly related to the free surface vertical velocity (FSVV) through the wave celerity, ω/k, in fact for a single sinusoidal wave:

$$\frac{1}{\omega}\frac{\partial z}{\partial t} = \frac{1}{k}\frac{\partial z}{\partial x} \tag{1}$$

and this allows an easy transformation from a time series of free surface elevation to the one of local wave slope.

Though this is strictly true only for linear waves and on a wave to wave basis, given free surface continuity and according to Cauchy's intermediate value theorem, there are values of ω and k such that the relationship is verified for a wave that results from a sum of elementary components.

Due to the relationship between local wave steepness and free surface vertical velocity it was analysed whether in fact the good correlation between impact and the velocity still holds. The correlation was assessed and found to be good and thus, as shown in Figure 4 the impacts were analysed versus the FSVV maxima.

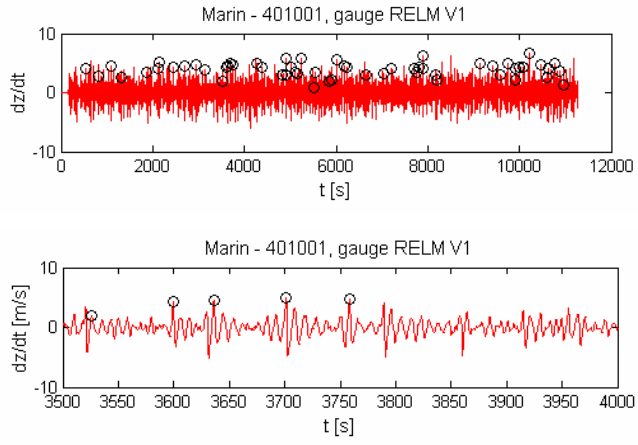

Figure 4.- Traced impacts versus time, superimposed on the free surface vertical velocity plot.

Because the resulting signal is non-linear, it is easier to calculate properties from the time trace and thus time traces are of interest. The passage from frequency to time domain, and vice-versa, is an easy step with the use of FFT algorithms.

PROBABILITY OF WAVE IMPACT

Figure 5 shows a relation between the crest height of the wave and the maximum vertical velocity or local slope. In red are shown the cases which resulted in wave slams. It can be observed that for higher values of maximum local slope the percentage of cases that led to impact increases. Therefore, fro a given sea state the probability of impact can be n«modelled as a function of the local wave slope.

In order to estimate the probability of having one impact given a sea state and the local free surface vertical velocity, written as:

$$P\left(Impact \middle| sea, w\right) \qquad (2)$$

the impacts within a sea state have been grouped and counted as a function of the free surface vertical velocity. An example of impact as function of FSVV and crest height is shown in Figure 5. The probability in (2) is then estimated as the number of impacts in one bin over the total number of waves that posses that FSVV. The bins have a finite width because of the discrete nature of the events.

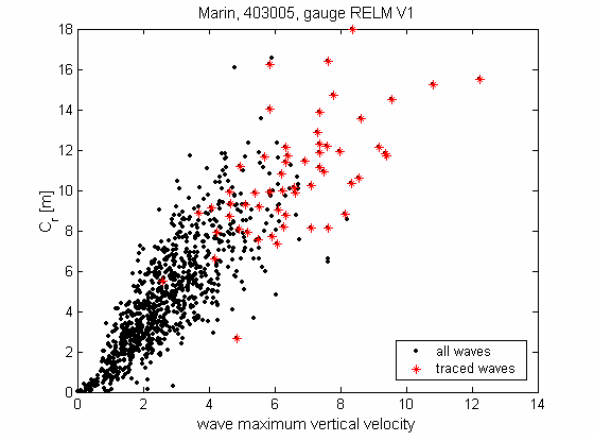

Figure 5.- Crest height as function of wave vertical velocity.

In order to determine a continuous function describing the probability of impact given a FSVV, a straight line was adjusted, in the sense of least squares, to the probability within the bin intervals in the region whose sum of probability exceeds roughly 3% till the value of 100%. Examples of the adjustment are shown in Figure 6 to Figure 8 and appear adequate.

In cases such as Figure 6, the 100% value was assumed to happen, though velocities were not high enough and uncertainty makes the last bin smaller than expected.

Given the repeated simulations of the same seastate, some scatter is evident in Figure 9. It appears there is some concentration of lines of the first group of tests to the left of the plot while group 2 and 3 concentrate more to the right. Due to the large uncertainty when characterizing such a complex event, it was decided that one weighted curve shall be used for the whole of the sets. The mean curve of the values given in Table 5 shall be used in further calculations.

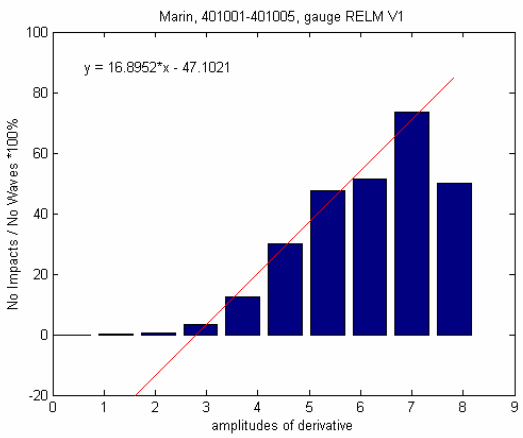

Figure 6.- Probability of impact versus free surface vertical velocity, average for group 1.

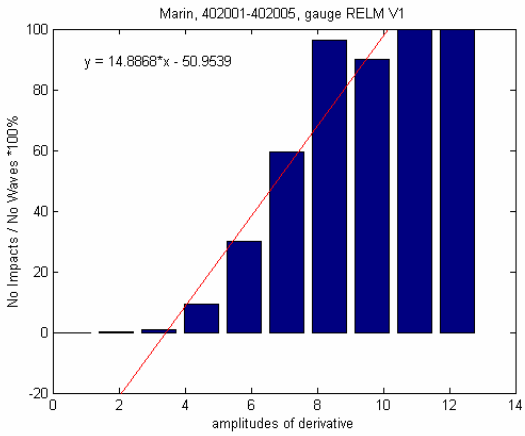

Figure 7.- Probability of impact versus free surface vertical velocity, average for group 2.

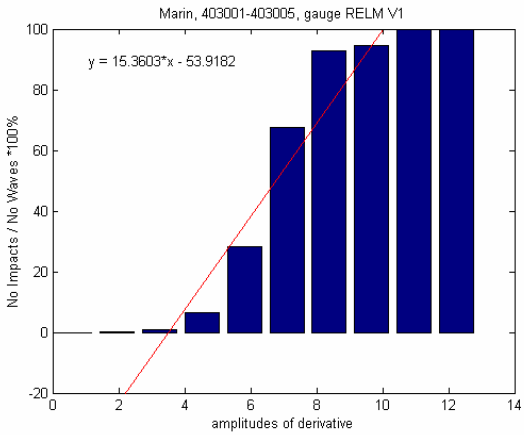

Figure 8.- .- Probability of impact versus free surface vertical velocity, average for group 3.

P(Impact|sea, w) = a.dz/dt+b [%]					
Hs = 8m Tp = 8s		Hs = 12m Tp = 12s		Hs = 14m Tp = 14s	
a	b	a	b	a	b
17.3	-39.9	20.1	-79.2	22.8	-96.4
20.9	-63.7	25.1	-106	24.7	-112.1
20.5	-62	16.9	-62.4	22.4	-90
13.9	-34.5	19.3	-72.3	15.3	-53.1
16.4	-46.4	18.5	-67	20.4	-84.2

Table 5.- Curves for group 1, 2 and 3 of tests.

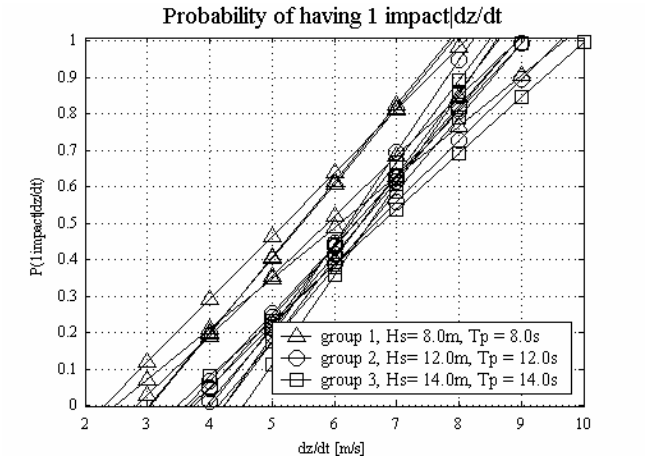

Figure 9.- Probability of impact given a free surface vertical velocity.

The closed form functional relationship that is derived for the average curve follows as:

$$P\left(Impact\middle|w\right)=0.19633\left(\left\langle w-3.631\right\rangle^{1}-\left\langle w-8.724\right\rangle^{1}\right) \quad (3)$$

It is possible to be more conservative by taking some other curve starting at lower velocities.

Because of the functional relationship between the probability of having an impact and the FSVV, it may be used directly to determine the long term probability of having an impact by evaluating the following expression over the scatter diagram:

$$P_{LT}\left(Impact\right)=\sum_{sea}\left[P\left(sea\right)\int_{0}^{\infty}P\left(Impact\middle|w\right)f\left(w\middle|sea\right)dw\right] \quad (4)$$

where $P\left(sea\right)$ is the probability of having a certain seastate and $f\left(w\middle|sea\right)$ is the probability density function of FSVV given that the seastate has occurred.

It is not absolutely correct to mix a discrete probability of impact given FSVV with a continuous distribution of FSVV, but it could be understood as taking the average velocity over an interval, the associated probability, and shrinking the interval to zero.

As in other long term evaluations, the number of cycles that the system endures under each sea state, in proportion to the total number of cycles, may be taken into account by a weighing factor in the kernel of the integral, i.e., greater average period gets less cycles. The usual form of this factor is:

$$wf=\frac{overall\ average\ period}{average\ period\ \ for\ the\ sea\ state} \quad (5)$$

In expression (4) the only missing element is the probability density function for the FSVV.

NUMERICAL SIMULATION OF WAVE TIMETRACES

In order to make more accurate calculations, a second order time trace is produced by using the method of Sharma and Dean (1981). The method results from second order wave theory as:

$$z\left(t\right)=\sum_{i=1}^{N}a_{n}\cos\left(\theta_{i}\right)+\frac{1}{4}\sum_{n=1}^{N}\sum_{m=1}^{N}a_{n}a_{m}\begin{bmatrix}1 & 1\end{bmatrix}\begin{bmatrix}\left(k_{n}+k_{m}\right)\cos\left(\theta_{n}+\theta_{m}\right)\\-\left|k_{n}-k_{m}\right|\cos\left(\theta_{n}-\theta_{m}\right)\end{bmatrix} \quad (6)$$

with

$$\theta_{i}=-\omega_{i}t+\xi_{i} \quad (7)$$

$$\xi_{i}\sim U\left[0,2\pi\right[\quad (8)$$

The use of FFT algorithm, the symmetry of the second order term and vector manipulation such that equal frequencies are summed before the transform is applied, makes it fast to transform the second order sum and difference frequency components into the second order time signal.

The time derivative is taken at the centre node of a sliding three point Legendre polynomial, which is a fast procedure due to vectorization of the algorithm, but it is also possible to write down the equation for the derivative of (6)itself and directly produce the signal derivative. The analogous physical procedure goes for the sensors used in collecting field elevation data because many times the elevation results from the integration of velocity or double integration of acceleration, that is the raw data the sensor actually produces, and thus the discrete time derivatives and their drawbacks, especially those related to signal noise, may be reduced by registering the raw data. When only elevation is available, then the sliding node derivative scheme is applicable to the signal after some tests have been made to the quality and odd points have been removed.

The numerical simulation is intended to replace further experimental tests if only the FSVV is needed and therefore the quality of the proposed second order approximation and also the benefits when compared to a linear simulation have to be assessed. The experimental tests themselves have to be compared against field data and validated.

In order to make a comparison between field data, basin data and numerical simulations, it is chosen to compare field data with numerical simulation and basin data with numerical simulation, eliminating direct comparison between field and basin data.

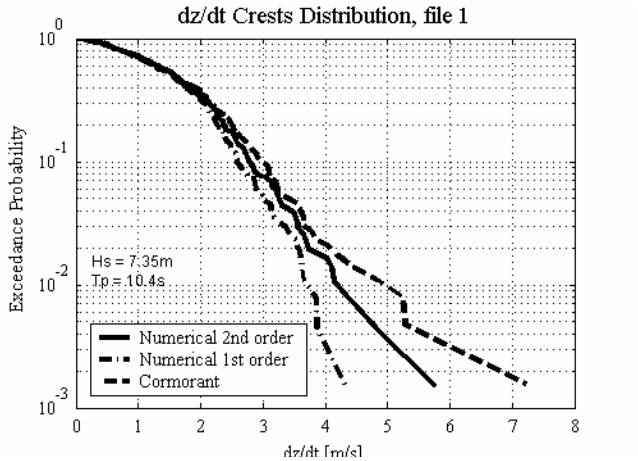

Figure 10.- Comparison of the cumulative probability of exceedance of field data and numerical simulation.

Field data used in this section originated from North Cormorant and were collected during a storm in 11th-12th March 1996. The time traces of free surface elevation consist of sequences with 34min duration at a 0.5s sampling period. Typical comparisons are shown in Figure 10 and Figure 11. In order to make fair comparison the numerical simulation was run with the same sampling period as the field data and thus the linear curves are not as smooth as would otherwise result from longer simulation time and smaller sampling period.

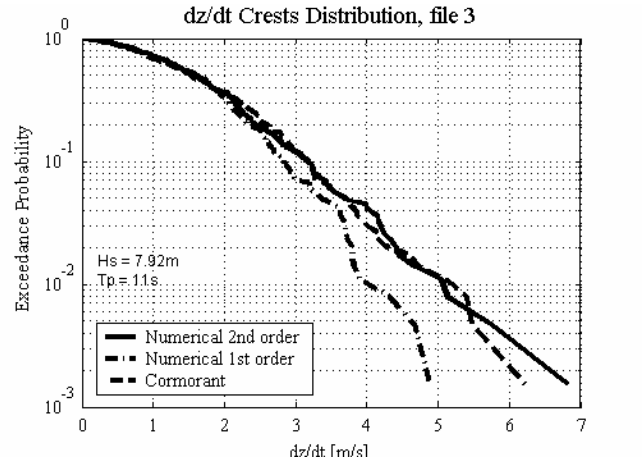

Figure 11.- Comparison of the cumulative probability of exceedance of field data and numerical simulation.

The relative error between the cumulative probability of exceedance of FSVV from basin simulations and numerical simulation has been calculated as:

$$e = \left| \frac{PexcNum - PexcBasin}{PexcBasin} \right| \qquad (9)$$

where the basin simulations are thus considered to be good representations of field data.

It may be seen in Figure 12 that the relative error for the first order simulation is increasing for large velocities and in fact the error is unity before the maximum velocities have been attained. The second order simulation is capable of reproducing the large velocities and for a typical simulation the error in the cumulative distribution function is about 10% at the maximum velocities.

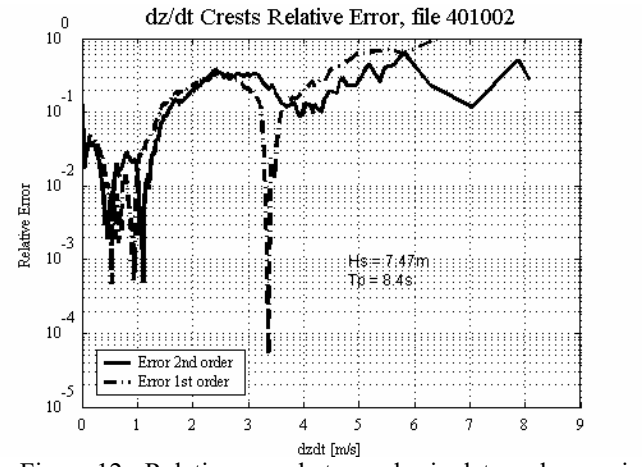

Figure 12.- Relative error between basin data and numerical simulation, Hs 8m, Tp 8s.

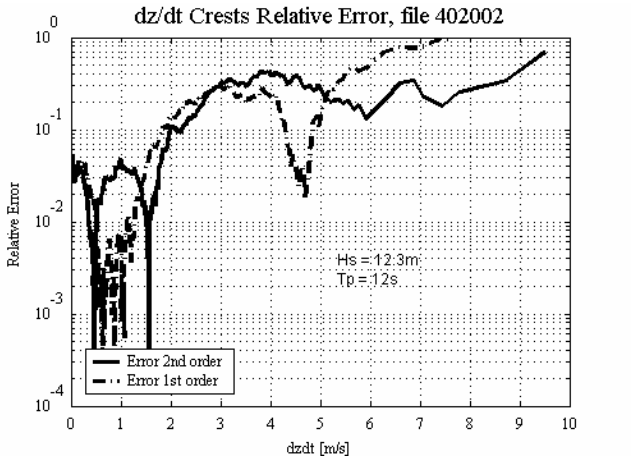

Figure 13.- Relative error between basin data and numerical simulation, Hs 12m, Tp 12s.

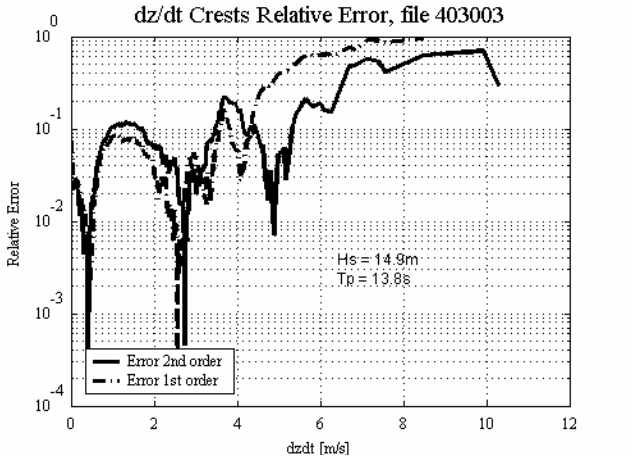

Figure 14.- Relative error between basin data and numerical simulation, Hs 14m, Tp 14s.

PROBABILITY OF IMPACT

To demonstrate the application of the approach proposed an example is given with a wave scatter diagram from an area in the North of Europe corresponding to the North Sea, whose scatter diagram's equiprobability contours are plotted in Figure 15. The procedure used was simply to calculate (4) with the probability density function of FSVV being determined from simulations of second order waves in relevant sea states chosen from the scatter diagram.

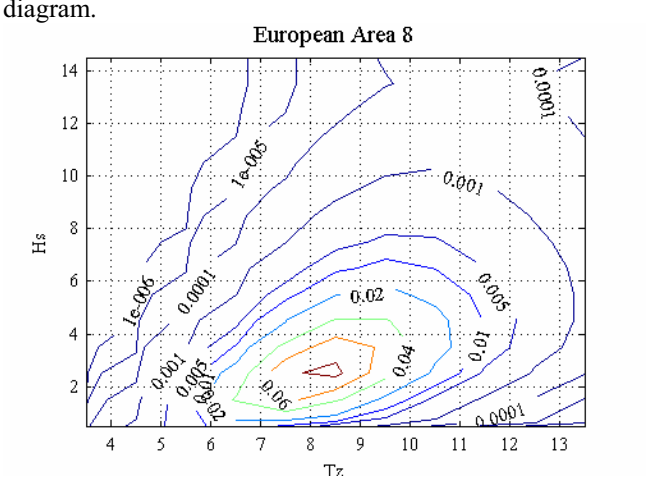

Figure 15.- Scatter diagram plot with contour probability levels for European area corresponding to North Sea.

The parameters for the simulated sea states are presented in Table 7. The parameters were estimated from the resulting second order time traces whilst in Table 7 are those given as input data. The input data are actually referred to the first order values determined for a JONSWAP spectral representation with different values of the peak enhancement factor γ.

γ = 1.0, 2.0, 3.3		
Hs [m]	Tp [s] (= 1.4 Tz)	Tz [s]
6	7.14, 10.36, 12.18	5.1, 7.4, 8.7
8	7.98, 9.8, 11.9, 14.0	5.7, 7.0, 8.5, 10.0
10	8.96, 10.92, 13.44, 15.68	6.4, 7.8, 9.6, 11.2
12	9.8, 12.04, 13.16, 14.7, 17.36	7.0, 8.6, 9.4, 10.5, 12.4
14	10.5, 12.74, 14.0	7.5, 9.1, 10

Table 6.- Simulated sea states of the European area, values given as input to the second order simulation.

γ = 1.0, 2.0, 3.3	
Hs [m]	Tp [s]
6	7, 10, 12
8	8, 10, 12,14
10	9, 11, 13,15
12	10, 12, 13,1 4, 17
14	10, 13, 14

Table 7.- Simulated seastates of the European area ,

The calculation was performed for the three values of γ. It was assumed that the given sea states are representative of the values of the FSVV for Hs greater than or equal to 5.5m. The probability of having these sea states was augmented such that the sum gave 1 while maintaining the relative values.

The probability of having Hs greater than or equal to 5.5m was determined from the scatter diagram of European area 8 and gave a value of 0.1627. This value is constant for all γ and multiplied the values of probability of impact calculated with the chosen sea states.

The probability of having one impact given, at least, the specific bow geometry, the European area 8 scatter diagram, the second order simulations and head waves, are presented in Table 8.

γ	$P_{LT}(Impact\|Hs>=5.5)$	$P_{LT}(Impact)$
1.0	0.0074	0.0012
2.0	0.0059	0.00096
3.3	0.0048	0.00078

Table 8.- Probability of impact for European area 8.

POSITION OF IMPACT RELATED TO CREST HEIGHT

Besides the probability of the impacts, the position of the impacts, their characteristics (magnitude, characteristics in time, spatial extent, effect of bow shape) and resulting structural responses are important. In the SAFE-FLOW project a complete methodology has been developed to derive this, see Figure 16 (Voogt, 2004).

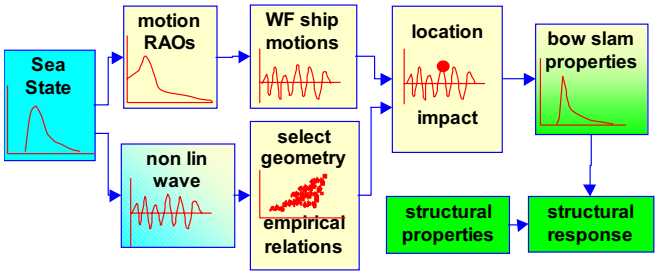

Figure 16.- Complete wave impact prediction methodology

In this paper the position of the impacts will be discussed. The impact characteristics (magnitude, characteristics in time, spatial extent, effect of bow shape) are present elsewhere, see (Voogt, 2004) and (Voogt and Buchner, 2004).

In the model an array of pressure transducers was installed. In total 5 columns of each 8 sensors were available for the analysis. From the repeated wave tests it was found that large spreading can occur on the time trace of the pressure in exactly reproduced waves. Therefore the impulse of the slam is calculated with an integration of the pressure over its duration. The magnitude of the impulses is plotted for a column of transducers, see Figure 17.

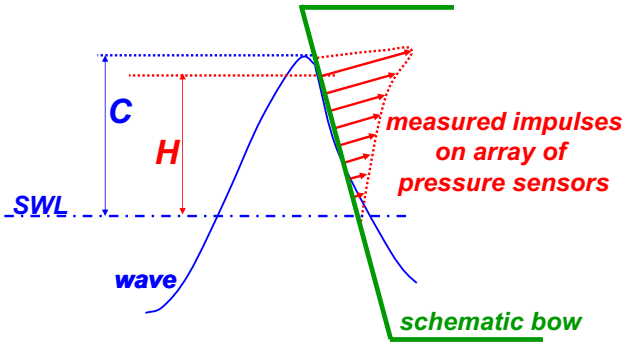

Figure 17.- Definition of slam centre (H) with respect to crest height (C) of incoming undisturbed wave

From this column of measured impulses the slam centre (H) can be defined as the level above the free surface with the maximum impulse. This height can be compared with the crest height of the corresponding incoming wave (C). Figure 18 shows this comparison for the crest heights of the undisturbed waves compare to the slam centre.

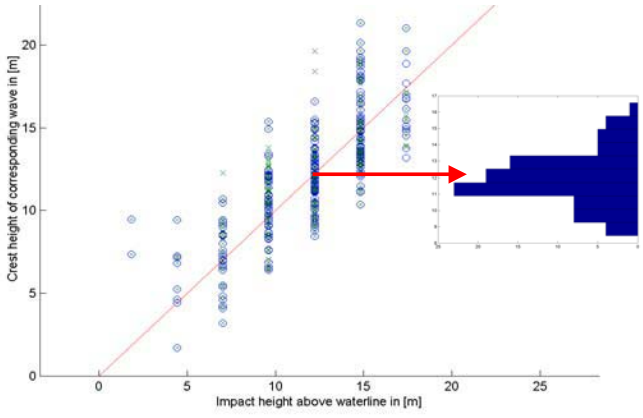

Figure 18.- Slam centre (H) on horizontal axis as function of crest height (C)

Due to the adopted method the impact height above the waterline is sampled with the distance between the rows of the transducers. For each impact with the slam centre at the third row from above a histogram of corresponding crest heights is shown with a small inset to the graph. It is clear that some spreading occurs but that most of the crest heights do correspond to the slam centre. The comparison with the wave heights of the incoming undisturbed waves show that most slam loads occur relatively close to the wave crest. This is consistent with the observation that the maximum velocity occurs close to the crest front of the incoming wave.

POSITION OF IMPACT RELATED TO SHIP MOTIONS

The previous section showed that the slam centre occur close to the crest of the undisturbed non-linear wave. However for the design of a bow panel in a floating structure, also the ship motions should be taken into account. To check the assumption that these motions in steep waves can still be described with linear diffraction theory, the model tests reported with a floating model (Voogt, 2001) were analysed further.

An iterative procedure has been developed that fits a linear wave and its second-order contributions to a measured wave train. The procedure works as follows:

1. An estimate of the linear part of the wave train is given. In practice, a good first guess is the measured wave train itself.
2. With a Discrete Fourier Transform (DFT) the amplitudes and phases of the linear estimate are determined.
3. The corresponding second-order sum- and difference frequency wave is determined and added to give an estimate of the total wave.
4. The difference between the estimated wave and the measured wave is determined. If this difference is larger than a certain pre-defined value, the difference is added to the linear estimate and the scheme is repeated from point 2 onwards.

The sum and difference-frequency waves are not determined for the entire, theoretical frequency range. Both are restricted to the frequency range [0, ω_{max}], where the cut-off frequency ω_{max} depends on the wave spectrum. A second-order fit is not realistic above the cut-off frequency since third- and higher order effects are bound to occur. The exact formulation for the cut-off frequency (or cut-off wave number k_{max}) is taken from (Stansberg, 1998) and equals:

$$k_{max}A_{max,R} < 2;$$

$$A_{\max,R} = \sigma\left[\sqrt{(2\ln n)} + \frac{0.577}{\sqrt{(2\ln n)}}\right] \qquad (10)$$

Where σ is the standard deviation of the wave record and n the number of independent amplitudes, estimated as:

$n = \frac{T}{T_z}$; T_z is the zero-upcrossing period and T the duration of the signal (NΔt).

For the waves considered so far, this iterative scheme is found to converge reasonably fast. The break-of criterion for the iterative scheme is chosen as follows:

$$\frac{\max\left(\left|estimated \quad wave - measured \quad wave\right|\right)}{\max\left(\left|measured \quad wave\right|\right)} < \varepsilon \qquad (11)$$

A threshold value ε of 0.01 was used in the examples shown in this document.

After the scheme has converged, the linear amplitudes ς_i are known and the response to this linear wave can be calculated. The table below shows a comparison of the standard deviations from the calculation and the measurements for a head seas condition.

	measurement	Linear calculation
Wave [m]	3.63	3.62
Surge [m]	1.00	0.96
heave [m]	1.50	1.32
pitch [deg]	2.26	2.04

Table 9.- Measured vessel response compared to calculated response assume linear theory.

A good comparison between measurements and linear calculations is found, which is confirmed in the time traces in Figure 19.

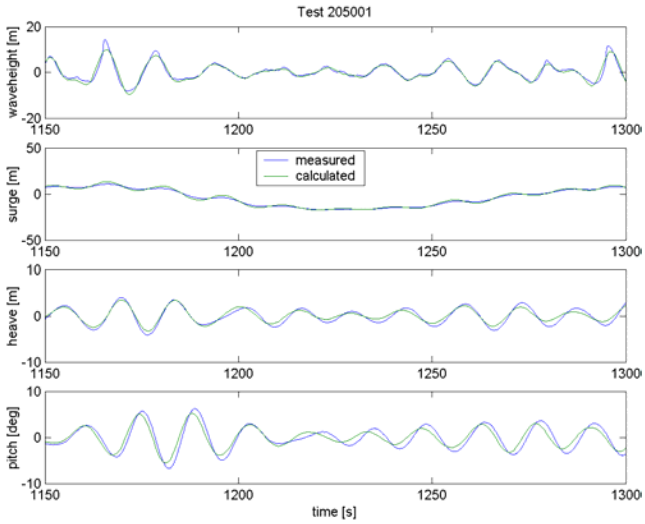

Figure 19.- Time traces of measured vessel response compared to calculated response assuming linear motion response

Even for these large differences between the linear wave and the measured wave, the linear wave is still capable to describe the major part of the ship response. Therefore the following procedure is implemented to determine the location of the impact:

- For a time trace of the linear wave the motions of the vessel are calculated.
- With this linear wave non-linear wave components can be calculated and added to the time traces.
- Combining the time trace of the non-linear wave and the linear ship motions gives a relative wave motion in front of the vessel.
- From these relative motions the slam centre can be determined if a slam occurs.

CONCLUSIONS

Based on the results presented, the following conclusions seem justified:

The free surface vertical velocity is a good identifier for wave impacts on FPSO bows.

The second order formulation for determining the free surface vertical velocity is adequate for the type of problem at hand whilst linear solutions are not.

The possibility of running long second order numerical simulations may be used in order to give not only the parameters but also coherent confidence intervals.

Adjusting a theoretical distribution, and checking the confidence interval a priori, makes the method fast and less prone to error.

The position of the impact is determined by the non-linear wave crests and the ship motions. The ship motions can be determined based on a linear response to the non-linear waves considered.

ACKNOWLEDGEMENTS

The SAFE-FLOW project (SAFE-FLOating offshore structures under impact loading of shipped green water and Waves) is funded by the European Community under the 'Competitive and Sustainable Growth' Programme (EU Project No.: GRD1-2000-25656) and a group of 26 industrial participants (oil companies, shipyards, engineering companies, regulating bodies). The participants are acknowledged for their interesting discussion of the results during the project and the permission to publish the present paper. The authors are solely responsible for the present paper and it does not represent the opinion of the European Community.

REFERENCES

Buchner, B., 1998, "A New Method for the Prediction of Non-Linear Relative Wave Motions", *Proceedings of the 17th International Conference on Offshore Mechanics and Arctic Engineering*, ASME, New York, paper OMAE98/SR-0592.

Buchner, B., 2002, *Green Water on Ship-type Offshore Structures,* PhD-thesis Delft University of Technology, 2002.

Guedes Soares, C.; Fonseca, N., and Pascoal, R., 2001, "Experimental and Numerical Study of the Motions of a Turret Moored FPSO in Waves", *Proceedings of the 20th International Conference on Offshore Mechanics and Arctic Engineering (OMAE'01);* ASME, New York, Paper OMAE2001/OFT-1071.

Guedes Soares, C., Pascoal, R., 2002, "Experimental Study of the Probability Distributions of Green Water on the bow of Floating Production Platforms", *Proceedings of the 21st International Conference on Offshore Mechanics and Arctic Engineering (OMAE2002)*, ASME, New York, paper OMAE2002-28626.

Hellan, Ø., Hermundstad, O.A., Stansberg, C.T., 2001, "Design Tool for Green Sea, Wave Impact, and Structural Response on Bow and Deck Structures", *Offshore Technology Conference*, Paper OTC 13213, Houston, Texas, U.S.A.

Sharma, J. N. and Dean, R. G., 1981, "Second-Order Directional Seas and Associated Wave Forces", *J. Soc. Petroleum Engineering*, 4, pp 129-140.

Stansberg, C. T., 1998, "Non-Gaussian Extremes in Numerically Generated Second-Order Random Waves on Deep Water", *Proceedings of the Eighth International Offshore and Polar Engineering Conference*.

Voogt, A.J., 2001, "Discussion Problem Identification, SAFE-FLOW project", *MARIN Report No. 15874-1-OB*, Wageningen, The Netherlands.

Voogt, A.J., 2004, "Prediction of Wave Impact Loading, SAFE-FLOW project", *MARIN Report No. 15874-1-SMB,* Wageningen, The Netherlands.

Voogt, A.J., and Buchner, B., 2004, "Wave impact excitation on ship-type offshore structures in steep fronted waves", *Proceedings OMAE Speciality Conference on Integrity of Floating Production, Storage & Offloading (FPSO) Systems,* Houston August-Spetember 2004, Paper OMAE-FPSO'04-0062